Near-field propagation of tsunamis from megathrust earthquakes

GEOPHYSICAL RESEARCH LETTERS, VOL. 34, L14316, doi:10.1029/2007GL030494, 2007

Near-field propagation of tsunamis from megathrust earthquakes

John McCloskey,[1] Andrea Antonioli,[1] Alessio Piatanesi,[2] Kerry Sieh,[3] Sandy Steacy,[1] Suleyman S. Nalbant,[1] Massimo Cocco,[2] Carlo Giunchi,[2] Jian Dong Huang,[1] and Paul Dunlop[1]

Received 25 April 2007; revised 15 June 2007; accepted 25 June 2007; published 27 July 2007.

[1] We investigate controls on tsunami generation and propagation in the near-field of great megathrust earthquakes using a series of numerical simulations of subduction and tsunamigenesis on the Sumatran forearc. The Sunda megathrust here is advanced in its seismic cycle and may be ready for another great earthquake. We calculate the seafloor displacements and tsunami wave heights for about 100 complex earthquake ruptures whose synthesis was informed by reference to geodetic and stress accumulation studies. Remarkably, results show that, for any near-field location: (1) the timing of tsunami inundation is independent of slip-distribution on the earthquake or even of its magnitude, and (2) the maximum wave height is directly proportional to the vertical coseismic displacement experienced at that location. Both observations are explained by the dominance of long wavelength crustal flexure in near-field tsunamigenesis. The results show, for the first time, that a single estimate of vertical coseismic displacement might provide a reliable short-term forecast of the maximum height of tsunami waves.
Citation: McCloskey, J., A. Antonioli, A. Piatanesi, K. Sieh, S. Steacy, S. S. Nalbant, M. Cocco, C. Giunchi, J. D. Huang, and P. Dunlop (2007), Near-field propagation of tsunamis from megathrust earthquakes, *Geophys. Res. Lett.*, *34*, L14316, doi:10.1029/2007GL030494.

1. Introduction

[2] The great magnitude 9.2 Sumatra-Andaman earthquake of 26 December 2004 produced vertical seafloor displacements approaching 5 m above the Sunda trench southwest of the Nicobar Islands and offshore Aceh [*Subarya et al.*, 2006; *Vigny et al.*, 2005; *Piatanesi and Lorito*, 2007; *Chlieh et al.*, 2007] creating a large tsunami that propagated throughout the Indian Ocean, killing more than 250,000 people. Waves incident on western Aceh reached 30 m in height. On March 28 2005 the megathrust ruptured again in the magnitude 8.7 Simeulue-Nias earthquake but in this case the waves nowhere exceeded 4 m and few people were killed by them. The Simeulue-Nias earthquake nucleated in an area whose stress had been increased by the Sumatra-Andaman earthquake [*McCloskey et al.*, 2005]. Follow-up studies [*Nalbant et al.*, 2005; *Pollitz et al.*, 2006] show that it has additionally perturbed the surrounding stress field and has, in particular, brought the megathrust under the Batu and Mentawai Islands closer to failure. Recent aseismic slip [*Briggs et al.*, 2006] has further increased the stress (Figure 1). Paleogeodetic studies show that the megathrust under the Batu Islands is slipping at about the rate of plate convergence [*Natawidjaja et al.*, 2004] while under Siberut Island it has been locked since the great 1797 earthquake and has recovered nearly all the strain released then [*Natawidjaja et al.*, 2006].

[3] The contrasting 2004 and 2005 events highlight the difficulties attendant on preparing coastal communities for the impact of tsunamis from earthquakes whose slip-distributions and even magnitudes are essentially unknowable even where, as is the case on the Sunda megathrust to the west of Sumatra, there is clear evidence of an impending great earthquake. Cities on the west coast of Sumatra, notably Padang and Bengkulu with combined populations in excess of 1 million, lie on low coastal plains and are particularly threatened by tsunamis generated by Mentawai segment earthquakes. Here we attempt to understand these threats by simulating tsunamis which would result from a wide range of plausible earthquakes sources.

2. Modelling Scheme

[4] Our simulations, which will be described in detail elsewhere, combine sophisticated numerical modelling with the best current geologically-constrained understanding of the state of the Sunda megathrust to forecast the range of possible tsunamis which might be experienced following the next great Mentawai Island earthquake. We define four likely fault segments which are suggested by the structural geology of the megathrust, by historical earthquakes and by long-term and recent stress accumulation. All simulated earthquakes are on the same 3D structure. The Sunda trench in the area of interest is approximately linear, strikes at about 140° and extends from the equator to about 6.5°S. The plate interface dips at about 15° resulting in a down-dip seismogenic width of about 180 km. We simulate about 100 or so complex slip distributions, around 25 for each fault segment length, which have been judged, by reference to paleoseismic and paleogeodetic data, to be likely candidates for the future event [see, e.g., *Briggs et al.*, 2006; *Prawirodirdjo et al.*, 1997]. We make no assumptions about the location of maximum slip on the fault, whether shallow near the trench or deep under the volcanic arc, but the slip models conform to the observed fractal distribution [*Mai and Beroza*, 2002] though our main results are not sensitive to a wide range of plausible slip distributions. We note that these slip distributions conform to constraints on the gradient of slip which are set by material and constitutive properties of the lithosphere and have been used elsewhere to model slip heterogeneity in tsunamigenesis [*Geist*, 2002].

[1] Geophysics Research Group, School of Environmental Sciences, University of Ulster, Coleraine, Northern Ireland.
[2] Seismology and Tectonophysics Department, Istituto Nazionale di Geofisica e Vulcanologia, Rome, Italy.
[3] Tectonics Observatory, California Institute of Technology, Pasadena, California, USA.

0094-8276/07/2007GL030494$05.00

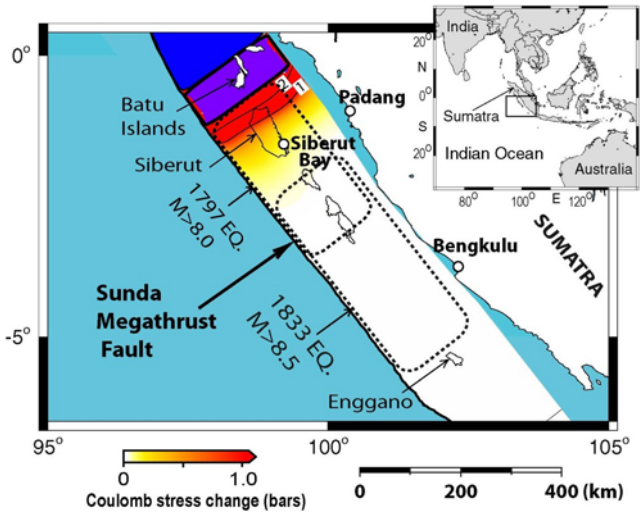

Figure 1. Historical earthquakes and current interaction stresses on the Sunda megathrust. Dotted lines indicate outlines of main historical earthquake ruptures as estimated by paleogeodetic studies. Dark blue indicates the southern extent of the 2005 earthquake. Current interaction stresses, shown in the yellow-red colour scale, have been calculated for this study and include coseismic stress and both the effect of afterslip on the Simeulue-Nias source region and aseismic slip under the Batu islands, shown in purple. Under and to the north west of Siberut Island where interaction stresses are large, the megathrust is advanced in its seismic cycle and all synthetic earthquakes nucleate here. South of Siberut, the subduction zone has not failed since 1833, implying the potential for a rupture to propagate more than 600 km south-eastward from about 0.5°S. White circles indicate locations of simulated tide gauges discussed in the text.

Using a finite-element model of the elastic structure of the lithosphere customised for the western Sumatran forearc and including the effects of topography, we calculate the seafloor displacements which would result from each selected slip distribution. These displacements define boundary conditions for the tsunami simulation. The non-linear shallow water equations are solved numerically using a finite difference scheme on a staggered grid [*Mader*, 2004]. The initial sea-surface elevation is assumed to be equal to the coseismic vertical displacement of the seafloor calculated using the elastic model, and the initial velocity field is assumed to be zero everywhere [*Satake*, 2002]. We apply a pure reflection boundary condition along the true coastline at which the depth has everywhere been set to 10 m to avoid numerical instabilities. This boundary condition ensures that all the tsunami kinetic energy is converted into potential energy at the coast and thus, while we do not simulate the complex processes of inundation which are controlled by fine scale details of the near-shore topography, our predicted coastal wave heights include both the effect of shoaling to 10 m depth and the interaction with the solid boundary.

3. Results

[5] We report on the systematic control of tsunami waveforms in the near-field, formally defined here as that region which experiences vertical co-seismic displacement which is measurable with current GPS technology. We find that the shape of the tsunami wave train recorded at any tide gauge is, to first order, independent of the slip-distribution or even of the magnitude of the earthquake that caused it. Figure 2 illustrates this independence with respect of two very different simulated Mentawai earthquakes. Event I is a 330 km long re-rupture of the 1797 segment and with magnitude 8.3 while Event II is a 630 km rupture of both the 1797 and 1833 segments with magnitude 9.0. Despite the great difference in both magnitude and location of high slip regions in the rupture with respect to the tide gauge, the shapes of the wave-height time-series are different only in detail; the timing of the main tsunami phases is constant. Conversely, the maximum height of the waves differs by an order of magnitude. This similarity, which is observed for all 100 simulations at all simulated tide gauges, allows the accurate prediction of the arrival time of flooding phases. The first wave crest, for example, arrives at Padang 33.5 ± 2.5 (2σ) minutes after the event origin. Similar predictions can be made for the other five near-field tide gauges in this study.

[6] Another feature of these curves is the visual similarity of the *z*-component of coseismic deformation experienced at the tide gauges, as indicated by the intercept on the height axes, despite the axes being scaled for the maximum height of the wave and not for the intercept; the ratio of coseismic displacement to maximum wave height is constant for these two events. Surprisingly, this observation is robust for all simulations and for all simulated tide gauges. Figure 3 shows the relationship between near-field vertical coseismic displacement and maximum observed tsunami height for three stations. This relationship holds for the other three tide gauges in the study though the scatter on the data is significantly higher for stations to seaward of the Islands. The coseismic displacement also predicts the depth of the deepest tsunami trough. Note that these results are not related to Plafker's rule of thumb [*Okal and Synolakis*, 2004], which is, incidentally, reproduced in this study, relating the maximum slip on the fault to the maximum observed wave height. These results show that the local tsunami energy is controlled by the local coseismic deformation, rather than the maximum deformation which may occur at many hundreds of kilometres distance and which generally do not predict the local tsunami at any specific point.

4. Discussion and Conclusions

[7] The explanation for these relationships is straightforward. The entire near-field region experiences a well defined pattern of vertical coseismic deformation, upward under the forearc high and downward under the forearc basin and the Sumatran coast, which is controlled by the geometry of the subduction interface, and which is extended laterally along the length of the rupture (Figure 4a). Whereas the amplitude of this wave varies strongly with the earthquake, to first order, the wavelength is always about 300 km and its ends, where vertical coseismic deformation is zero, are fixed at the trench and just landward of the coast (Figure 4b). These features are largely independent of the slip-distribution or magnitude of the event, for the great ($M > 8$) earthquakes considered in this study. Since the initial tsunami waves are driven by the coseismic seafloor

displacement their initial locations are controlled by this instantaneous long wavelength crustal flexing, no matter what its amplitude, and propagate perpendicularly to the strike of the megathrust in the near field. Wave phase velocities are controlled by bathymetry and the observed waveforms at every site are, therefore, also largely independent of the details of the causal event.

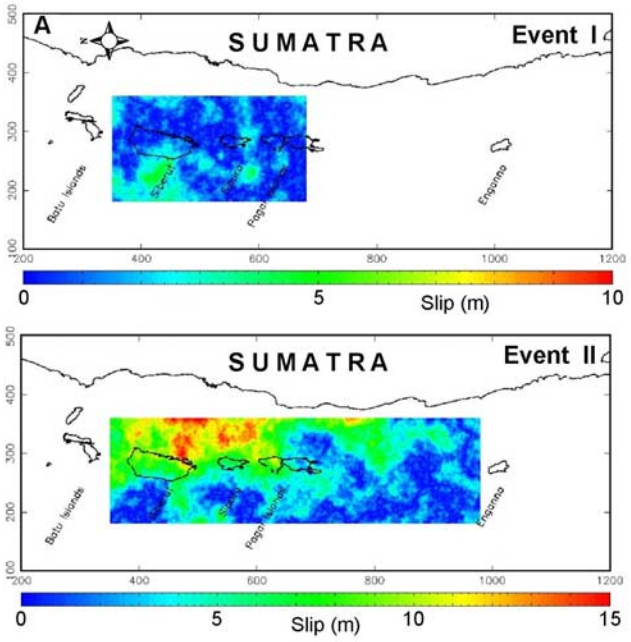

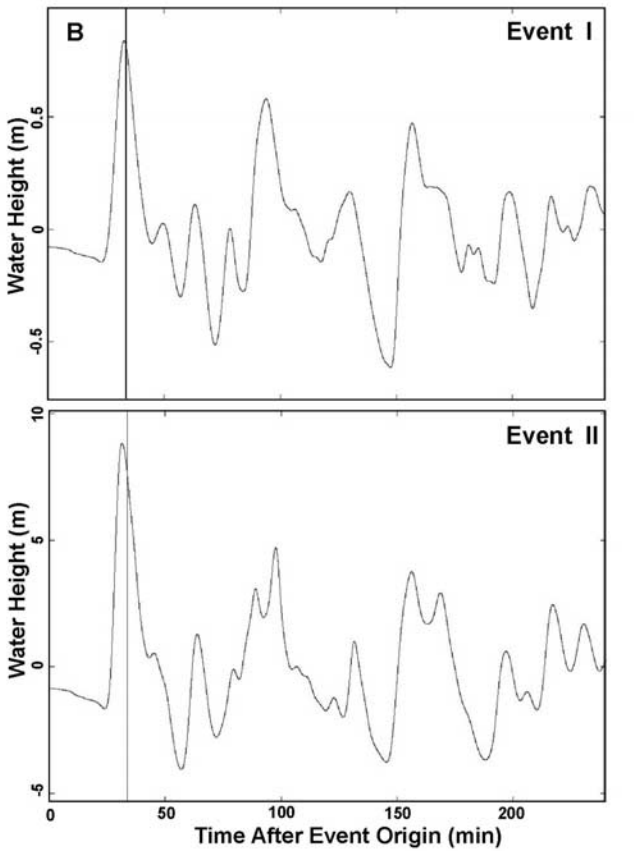

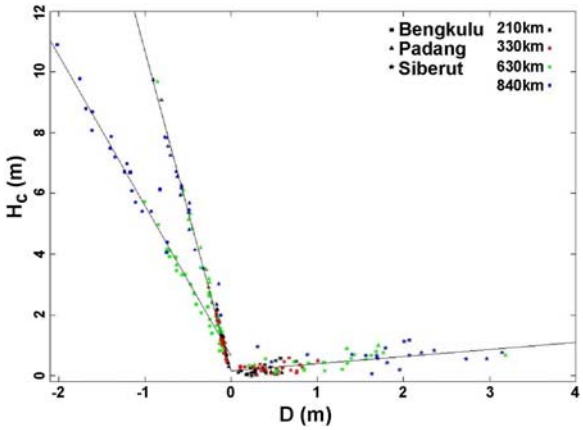

Figure 3. Vertical component of the coseismic displacement, D, at three locations against the height, Hc, of the highest wave experienced as would be recorded by a local tide gauge. Bengkulu is only in the near-field for 630 km and 840 km earthquakes. Coseismic uplift on the forearc islands evident here, for example, at Siberut Bay and its significant associated reduction in tsunami heights experienced there adequately explains the relatively low fatalities here during the 2004 and 2005. The opposite effect is evident at Padang and Bengkulu on the Sumatran coast. Lines show least squares fit to the data. The intercepts and slopes of these lines are controlled by the location of the station on the deformation profile and the local bathymetry.

[8] The strong correlation between maximum wave height (and minimum trough depth) and the vertical coseismic displacement at any point can also be understood by reference to this long wavelength crustal flexure. Since local tsunamis propagate normal to the axis of deformation, tsunami energy at any point is controlled, again to first order, by the potential energy of the coseismic tsunami wave along a line perpendicular to this axis through the point of interest. The potential energy is therefore proportional to the integral of the coseismic seafloor movement. Now we have seen that the amplitude of this profile is strongly earthquake dependent, thus the height of the resulting tsunami depends strongly on the event. However, since the general shape of the deformation wave is fixed

Figure 2. Tsunamis simulated for two simulated Mentawai Islands earthquakes observed at Padang: Event I 330 km rupture with M ≈ 8.3, and Event II 630 km rupture with M ≈ 9.0. Note the widely different scales used for each pair of diagrams. (a) Slip distributions viewed looking vertically down on the slipping plane. Axes scales are in km. Maximum slip on Event I is 6.5 m and is located seaward of the forearc high, the maximum slip in Event II is 14.7 m and is located under the forearc basin near Padang. (b) Height of simulated waves for Padang. The heights are referenced to the geoid and start with a negative intercept corresponding to the coseismic deformation experienced at Padang. Vertical lines indicate the mean arrival time of the first peak for all 100 simulations.

both in wavelength and phase, an estimate of its amplitude at any point, ideally some distance from a node of the flexure, is a good first order predictor of the entire potential energy line integral and thus the amplitude of the resulting waves. Given the generality of this explanation we expect that the relationships reported in this paper will be applicable to any subduction zone though their details will be modified by local crustal geometry.

[9] These results may assist planning of preparedness strategies throughout the western Sumatran forearc complex. They show that the travel times of damaging tsunami phases in the near-field are subject to strong lower bounds, of about 30 minutes for the Sumatran coast and somewhat less for the off-shore islands, which are independent of the nature of the seismic source. Validation of these results using recent earthquakes is not straightforward. The accurate measurement of phase arrival times requires the operation of tide gauges with high-frequency sampling and are not available in western Sumatra for the recent earthquakes. Travel times simulated here are, however, consistent with field observations made after the 2004 tsunami (e.g., http://ioc.unesco.org/iosurveys) and by the low-frequency tide gauge in Sibolga following the 2005 event (P. Manurung, personal communication, 2006). These short travel times preclude the possibility of using ocean wide tsunami warning systems in preparedness planning for western Sumatra. On the other hand, the strong correlations between coseismic displacement and the height of the tsunami wave, which have been demonstrated here for failure of the Sunda megathrust under the Mentawai Islands, offer real hope of producing accurate short-term forecasts of tsunami height on the basis of a single GPS vertical coseismic displacement estimate which could be made in a few minutes following the earthquake origin [see also *Blewitt et al.*, 2006]. These correlations, of course, are valid only for tsunamigenesis by dip-slip failure on the megathrust without significant contributions from other processes such as submarine landslide or normal fault rupture in the hanging wall block which have been invoked to explain anomalous tsunami energy following other earthquakes [*Pelayo and Wiens*, 1992; *Heinrich et al.*, 2000]. They also assume that slip on the earthquake is rapid, unlike the slow 2006 Java earthquake which efficiently generated a large tsunami in the absence of strong shaking on shore. Recent and historical earthquakes in western Sumatra would appear to satisfy these conditions.

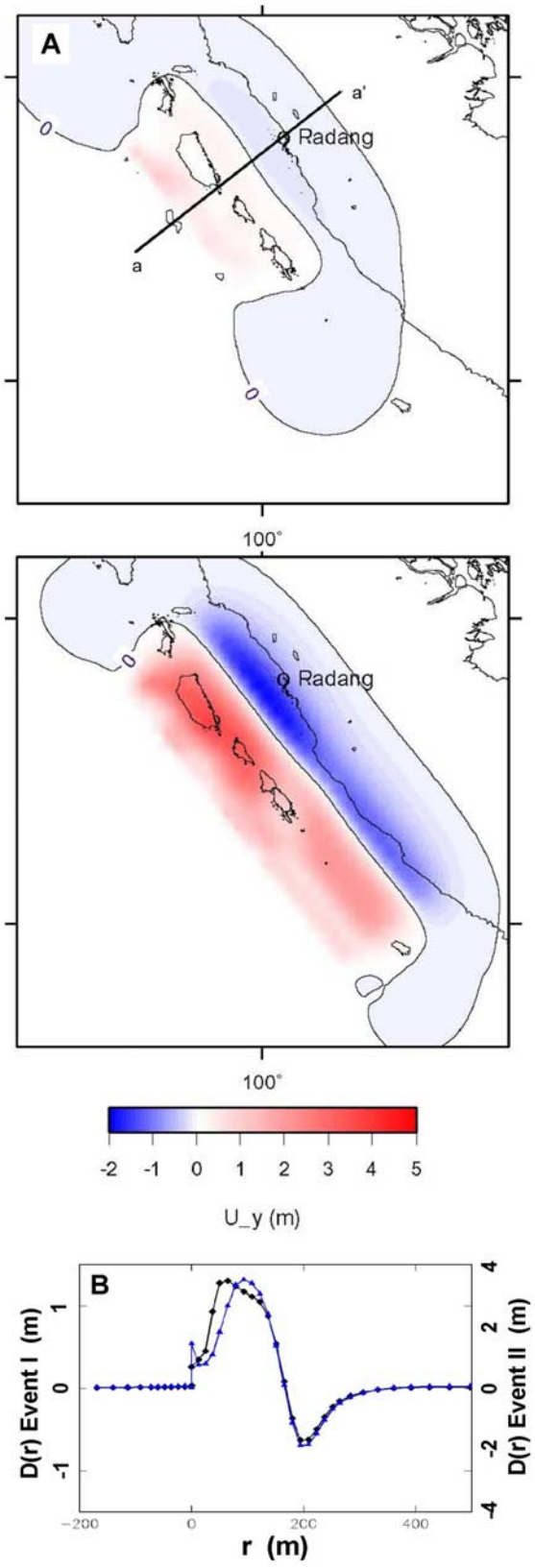

Figure 4. Vertical component of coseismic deformation. (a) Map view. Notice the similarity of the width and location of the emergent and subsiding zones, though the small difference in the location of maximum emergence, combined with the location of Siberut Island, suppresses the amplitude of the tsunami from the smaller event nonlinearly. (b) Vertical deformation along a-a' in Figure 4a. Distances, r, are measured in km from the trench. Event I, diamonds; Event II, triangles. Note different scales for the events. The step at r = 0 represents the surface rupture of the event. Deformation profiles are extremely smooth to landward where high-spatial frequency components of the slip distribution are filtered out by the 35 km or so of intervening crust. The greater scatter of the data close to the trench, for example for Siberut in Figure 3, is explained by the reduction in quality factor of this filter as the accretionary wedge thins toward the trench allowing more surface expression of the slip-complexity there.

[10] **Acknowledgments.** We thank Rory Quinn for assistance in the bathymetric modelling, Spina Cianetti for assistance in construction of the finite element model of subduction, and Chris Bean for constructive criticism of the manuscript. The Landsat ETM+ data is used courtesy of the Global Land Cover Facility (http://www.landcover.org). We acknowledge financial support from the Natural Environmental Research Council.

References

Blewitt, G., C. Kreemer, W. C. Hammond, H.-P. Plag, S. Stein, and E. Okal (2006), Rapid determination of earthquake magnitude using GPS for tsunami warning systems, *Geophys. Res. Lett.*, *33*, L11309, doi:10.1029/2006GL026145.

Briggs, R. W., et al. (2006), Deformation and slip along the Sunda megathrust in the great 2005 Nias-Simeulue earthquake, *Science*, *311*, 1897–1901.

Chlieh, M., J.-P. Avouac, V. Hjorleifsdottir, T.-R. A. Song, C. Ji, K. Sieh, A. Sladen, H. Hebert, L. Prawirodirdjo, Y. Bock, and J. Galetzka (2007), Coseismic slip and afterslip of the Great Mw9.15 Sumatra-Andaman Earthquake of 2004, *Bull. Seismol. Soc. Am.*, *97*(1A), S152–S173, doi:10.1785/0120050631.

Geist, E. L. (2002), Complex earthquake rupture and local tsunamis, *J. Geophys. Res.*, *107*(B5), 2086, doi:10.1029/2000JB000139.

Heinrich, P., A. Piatanesi, E. Okal, and H. Hébert (2000), Near-field modeling of the July 17, 1998 tsunami in Papua New Guinea, *Geophys. Res. Lett.*, *27*, 3037–3040.

Mader, C. L. (2004), *Numerical Modelling of Water Waves*, CRC Press, Boca Raton, Fla.

Mai, P. M., and G. C. Beroza (2002), A spatial random field model to characterize complexity in earthquake slip, *J. Geophys. Res.*, *107*(B11), 2308, doi:10.1029/2001JB000588.

McCloskey, J., S. S. Nalbant, and S. Steacy (2005), Indonesian earthquake: Earthquake risk from co-seismic stress, *Nature*, *434*, 291.

Nalbant, S. S., S. Steacy, K. Sieh, D. Natawidjaja, and J. McCloskey (2005), Earthquake risk on the Sunda Trench, *Nature*, *435*, 756–757.

Natawidjaja, D. H., K. Sieh, S. N. Ward, H. Cheng, R. L. Edwards, J. Galetzka, and B. W. Suwargadi (2004), Paleogeodetic records of seismic and aseismic subduction from central Sumatran microatolls, Indonesia, *J. Geophys. Res.*, *109*, B04306, doi:10.1029/2003JB002398.

Natawidjaja, D. H., K. Sieh, M. Chlieh, J. Galetzka, B. W. Suwargadi, H. Cheng, R. L. Edwards, J.-P. Avouac, and S. N. Ward (2006), Source parameters of the great Sumatran megathrust earthquakes of 1797 and 1833 inferred from coral microatolls, *J. Geophys. Res.*, *111*, B06403, doi:10.1029/2005JB004025.

Okal, E., and C. Synolakis (2004), Source discriminants for near field tsunamis, *Geophys. J. Int.*, *158*, 899–912.

Pelayo, A. M., and D. A. Wiens (1992), Tsunami earthquakes: Slow thrust-faulting events in the accretionary wedge, *J. Geophys. Res.*, *97*, 15,321–15,337.

Piatanesi, A., and S. Lorito (2007), Rupture process of the 2004 Sumatra-Andaman earthquake from tsunami waveform inversion, *Bull. Seismol. Soc. Am.*, *97*(1A), S223–S231, doi:10.1785/0120050627.

Pollitz, F. F., P. Banerjee, R. Bürgmann, M. Hashimoto, and N. Choosakul (2006), Stress changes along the Sunda trench following the 26 December 2004 Sumatra-Andaman and 28 March 2005 Nias earthquakes, *Geophys. Res. Lett.*, *33*, L06309, doi:10.1029/2005GL024558.

Prawirodirdjo, L., et al. (1997), Geodetic observations of interseismic strain segmentation at the Sumatra subduction zone, *Geophys. Res. Lett.*, *24*, 2601–2604.

Satake, K. (2002), Tsunamis, in *International Handbook of Earthquake and Engineering Seismology*, edited by W. H. K. Lee et al., pp. 437–451, Academic, San Diego, Calif.

Subarya, C., et al. (2006), Plate-boundary deformation associated with the great Sumatra-Andaman earthquake, *Nature*, *440*, 46–51, doi:10.1038/nature04522.

Vigny, C., et al. (2005), Insight into the 2004 Sumatra-Andaman earthquake from GPS measurements in southeast Asia, *Nature*, *436*, 201–206, doi:10.1038/nature03937.

A. Antonioli, P. Dunlop, J. D. Huang, J. McCloskey, S. S. Nalbant, and S. Steacy, Geophysics Research Group, School of Environmental Sciences, University of Ulster, Cromore Road, Coleraine, County Derry BT52 1SA, Northern Ireland. (j.mccloskey@ulster.ac.uk)

M. Cocco, C. Giunchi, and A. Piatanesi, Seismology and Tectonophysics Department, Istituto Nazionale di Geofisica e Vulcanologia, Via di Vigna Murata 605, I-00143 Rome, Italy.

K. Sieh, Tectonics Observatory, California Institute of Technology, 1200 E. California Boulevard, Pasadena, CA 91125, USA.